

## Oxidation Kinetics of Carbon Blacks over 1300-1700 K\*

W. Felder, S. Madronich,† and D. B. Olson

AeroChem Research Laboratories, Inc.  
P.O. Box 12, Princeton NJ 08542

### I. INTRODUCTION

The oxidation of carbonaceous particulate matter is of wide practical concern in power generation and pollution reduction. Typically, in fuel-rich portions of combustion flames, OH radicals can be the major oxidizing species (1-3). However, in regions of combustors and in the exhaust where soot is present and OH concentrations are essentially negligible (regions in which particles spend the major portion of their lifetimes within a device), oxidation by excess oxygen is important. The work described here utilized an entrained flow reactor (a modified High Temperature Fast Flow Reactor, HTFFR) to determine the reactivity of two carbon blacks with O<sub>2</sub> in the 1300-1700 K range. A wide range of oxygen concentration was investigated while maintaining independent control of total pressure and flow velocity (particle residence time). A method and apparatus were developed for feeding particles to the HTFFR and assuring that particle sizes lie below specified limits.

### II. METHODS AND APPARATUS

The primary measurement is the number of moles of carbon converted to CO<sub>x</sub> (= CO + CO<sub>2</sub>) in a residence time,  $t$ . Collected gas samples were analyzed gas chromatographically to determine the amount of CO<sub>x</sub> evolved after the particle and oxidizer mixture had traversed the flow tube reactor at a temperature,  $T$ , in a time,  $t$ . For surface oxidation of monodisperse spherical particles, evolving CO<sub>x</sub> at the expense of particle size (4):

$$u(t) = 1 - (1 - (R_e S_0 t / 3)) ^3 \quad (1)$$

where:  $u(t) = (m_0 - m_t) / m_0$ , is the burnoff at time  $t$ ;  $m_0$  and  $m_t$  are the mass of carbon input (g/s) and the mass of carbon remaining unoxidized at time  $t$ , respectively

$R_e$  = the external surface oxidation reactivity coefficient, g cm<sup>2</sup> s<sup>-1</sup>, a function of [O<sub>2</sub>]

$S_0$  = specific surface area of unoxidized carbon particles, cm<sup>2</sup>/g

Equation 1 assumes that the oxidation is chemically controlled (i.e., diffusion is rapid compared to reaction), and that the surface reactivity is a function only of available area. In this work, it was shown that the assumptions of surface reaction and chemical control are valid. The possible change in surface reactivity with oxidation was not addressed; thus the  $R_e$  values are referred to the original surface area.

To determine  $u(t)$ , it is necessary to measure [CO<sub>x</sub>] for the experimental condition and [CO<sub>x(max)</sub>], the amount of CO<sub>x</sub> produced by complete particle oxidation. The [CO<sub>x(max)</sub>] gives  $m_0$  in the expression for  $u(t)$  and is obtained by replacing the N<sub>2</sub> diluent flow to the HTFFR with an equivalent O<sub>2</sub> flow, thus com-

\* This work supported by the U.S. Army Research Office, Contract No. OAG29-83-C-0023.

† Present address: National Center for Atmospheric Research, Boulder, CO.

pletely converting input carbon to  $\text{CO}_x$ . Measurement of  $[\text{CO}_x]$  at other than complete oxidation conditions (replacing part of the  $\text{N}_2$  flow with  $\text{O}_2$ ) gives  $(m_0 - m_x)$ . Frequent  $[\text{CO}_x(\text{max})]$  determinations were interspersed with the  $[\text{CO}_x]$  measurements.

The HTFFR described by Fontijn and Felder (5) was modified for this work. Optical observation ports in the reaction tube were eliminated, allowing the isothermal zone of the reactor to include between 50 and 70 cm of the overall 90 cm length of the tube, depending on the flow conditions used in the experiments. The reaction tubes (two different diameter tubes were used in the present work, a 4.5 cm i.d. mullite tube, and a 2.5 cm i.d. 998 alumina tube) were resistively heated in three separately controlled zones of  $\approx 30$  cm each with 0.127 cm diam Pt/40% Rh resistance wire. At the reaction tube exit a HeNe laser beam crossed the particle-laden flow; scattered laser light was detected perpendicular to the beam. A 10 cm diam filter support and filter were mounted in a downstream bypass line so that the entire flow could be routed through it to collect partially oxidized particles for subsequent surface area measurements.

Particle feed was from a 10 cm i.d., 40 cm long tumbling bed supported  $\approx 30^\circ$  from horizontal on two bearings. The particle bed charge consists of 90% (wt.) silica sand and 10% carbon black. A small  $\text{N}_2$  flow through the bed formed a carbon black aerosol, some of which entered a particle takeoff tube and flowed to a "settling chamber." Feed rates at the bed outlet of 1-100 mg/min ( $10^{-5}$  to  $10^{-4}$  moles C/s) were achieved. In the 15 cm i.d., 75 cm long settling chamber the flow was smoothed with a conically shaped flow straightener and slowed to  $\approx 0.5$  cm/s so that particle aggregates with aerodynamic diameters  $\geq 4 \mu\text{m}$  settled out of the flow. In some experiments, settling chamber flow speeds up to 2 cm/s were used; under these conditions, particle aggregates up to  $\approx 10 \mu\text{m}$  could have passed through the settling chamber. This range of particle sizes is below the size at which bulk diffusion affects the oxidation rate measurements.

The flow from the settling chamber entered the HTFFR reaction tube, where the major portion of the  $\text{N}_2$  diluent and  $\text{O}_2$  were added radially to the flow. The mass flow of carbon to the reactor indicated by  $[\text{CO}_x(\text{max})]$  measurements was 0.05-5.0 mg/min ( $10^{-7}$  to  $10^{-5}$  mol C/s), or about 5% of the output of the particle feeder. The remaining carbon black particles were collected in the settling chamber. The flow of  $\text{O}_2$  in the experiments ranged from  $5 \times 10^{-5}$  to  $5 \times 10^{-3}$  mol/s and always exceeded the molar "carbon" flow by a factor of at least 20; for measurements of  $[\text{CO}_x(\text{max})]$ , the oxygen flow was  $10^3$  to  $10^4$  times in excess of the "carbon flow."

Laser scattering was also used to obtain kinetic data by measuring the concentration of  $\text{O}_2$  required to consume all of the input carbon in exactly the residence time. The  $\text{O}_2$  flow to the reactor was progressively incremented while recording the scattered light intensity; a plot was made of relative (to  $[\text{O}_2] = 0$ ) scattered light intensity against  $\log [\text{O}_2]$ . The intensity decreased linearly on such plots as the particles were consumed; the curve went to zero at the value of  $[\text{O}_2]$  at which the input carbon was consumed in the burnup time,  $t_b$ . The burnup time is simply related to  $R_p$ . The  $R_p$  values obtained using the scattered light method were identical with those obtained using the gc method.

Partially oxidized particles were collected on the inline filter for surface area measurements which yield information on the physical mechanism of the oxidation process. An adsorption analyzer (Quantachrome MS-8) was used for  $\text{N}_2$  adsorption at 77 K, and the results were analyzed using the one point BET method (7). Specific surface area ratios were measured as a function of fractional burn-off,  $u$ , from  $u = 0$  (particles that have traversed the reactor with  $[\text{O}_2] = 0$ ) to  $u = 0.7$ .

The carbon blacks, Raven 16 (R16), a lampblack, and Conductex SC (CSC), a conducting black, were chosen to have a wide difference in initial specific surface area and iron impurity concentration. Both have "high" sulfur concentrations. The materials were donated by Columbian Chemical Corporation, Tulsa, OK, and their properties are summarized in Table I.

### III. RESULTS AND DISCUSSION

#### 1. Specific Surface Area Measurements

The interaction between  $O_2$  and the carbon black particles can occur between two extreme modes (4,7,8): (1) reaction on an external non-porous surface; (2) reaction within a completely porous mass. In the first extreme, a particle of constant density,  $\rho$ , is oxidized and its radius decreases with burnoff. In the second extreme, a porous particle of constant radius is oxidized internally and its density decreases with burnoff. The ratio of specific surface areas of the unoxidized and partially oxidized particles,  $S_0/S(t)$ , are given by (9):

$$\begin{aligned} S_0/S(t) &= (1-u)^{0.33} && \text{(constant density)} \\ S_0/S(t) &= (1-u) && \text{(constant radius)} \end{aligned}$$

Representative data for the two carbon blacks are compared with these functions in Fig. 1; the results indicate that the external surface area available for reaction increases in a manner consistent with a constant density (case 1 above) burning. The present measurements can thus be interpreted as the oxidation of non-porous spherical particles (assumed monodisperse) which react at constant density and with no change in particle number density.

#### 2. Oxidation Rates

Oxidation rates were measured over 1300-1700 K for R16 and 1400-1700 K for CSC, more than three decades of oxygen partial pressure (0.02-60 kPa) and total pressures ( $O_2 + N_2$ ) from 20 to 60 kPa. Particle residence times were varied from 50-800 ms. The majority of the data were obtained using the gc method; additional data were obtained using the laser scattering method. Representative burnoff data from the gc measurements, plotted against  $[O_2]$  are shown in Fig. 2. Figure 3 shows data obtained using the laser scattering diagnostic as discussed above from one experiment on CSC at 1580 K and a total pressure of 27 kPa.

There were no discernible total pressure effect on the measured  $[CO_x]$  yields over the approximately factor of two-to-three variation in total pressure covered at each temperature investigated, and no gas velocity effects over a factor of six at any temperature, nor did changing the reaction tube diameter from 2.5 to 4.5 cm have any effect. The measured burnoff depended only on reactor temperature,  $[O_2]$  and residence time.

The gc data were analyzed to extract  $R_e$  by rearranging Eq. 1:

$$R_e = (3/S_0 t) \cdot (1 - (1 - u)^{0.33})$$

Representative results are plotted in in Figs. 4 and 5. For the laser scattering measurements,  $u = 1$  when the scattered intensity is zero and

$$R_e = 3/S_0 t_0$$

where  $t_0$  is the residence time for complete burnoff at the  $[O_2]$  determined from plots such as Fig. 3. Values of  $R_e$  so determined are included in Figs. 4 and 5.

These observed surface reactivities are chemically controlled as can be seen by comparing the calculated diffusion limited and observed reactivities. For diffusion controlled reaction on a spherical particle of radius,  $r$  (4):

$$R_{e,o} = (\psi D/r) \cdot (C_0 - C_x) \quad (2)$$

where  $R_{e,o}$  = diffusion controlled reactivity based on external surface area,  $g \text{ cm}^{-2} \text{ s}^{-1}$

$\psi = (M_c/M_o \nu)$  where  $\nu$  is the molar stoichiometric coefficient for the gas and  $M_c/M_o$  is the molecular weight ratio of carbon to the reactant gas. For the present studies,  $C + 1/2 O_2 \rightarrow CO$ , and  $\nu = 1/2$ , with  $\psi = (12/32) \cdot 2 = 3/4$

$D$  = Binary diffusion coefficient of the oxidant gas,  $\text{cm}^2 \text{ s}^{-1}$ .

$C$  = mass density of the gas at the particle surface,  $C_x$ , and in the free stream,  $C_0$ ,  $g \text{ cm}^{-3}$ .

Thus, diffusion control (small values of  $R_{e,o}$ ) is favored by high pressure (low diffusion rates), large particle size, and high temperature (high surface reaction rates). For pure diffusion control, i.e., when the surface reaction rate is infinitely rapid,  $C_x \rightarrow 0$ . Figure 6 shows the range of  $R_{e,o}$  calculated from Eq. 2) with  $C_x = 0$  at the temperature and pressure extremes used in the present work (60 kPa and 1700 K) compared to the experimentally measured values. For the nominal particle diameters of the carbon blacks,  $\approx 10$ -100 nm, diffusion controlled rates are large and the reaction rate is controlled by surface chemistry processes. Figure 6 shows that even if aggregates as large as 100  $\mu\text{m}$  were present in the reactor (and the settling chamber ensures that they were not), bulk diffusion rates would still be  $\approx 10$  times larger than the observed reaction rates under the present experimental conditions. On this basis, mass transfer to the carbon black particles does not significantly affect the observed measurements.

In the absence of diffusion effects, the slopes of plots like Figs. 4 and 5 give the apparent reaction order in  $[O_2]$ . The reaction orders,  $n$ , lie between 0.6 and 0.8. Table II contains a summary listing of the values of  $R_e$  for the present experiments in the form  $\log R_e = \log R_0 + n \log [O_2]$ .  $R_0$  is a fitting constant with units of  $g \text{ cm}^{-2} \text{ s}^{-1} [O_2]^{-n}$ .

### 3. Discussion

Figures 2, 4, and 5 show comparisons of the observed  $u$  and  $R_e$  with the predictions of the Nagle and Strickland-Constable, NSC, formulation (10) which has been successful in describing the reactivity of several carbonaceous materials with  $O_2$ , especially at higher temperatures than those used here (10,11). From the plots it is clear that the present results are not well described by two site NSC kinetics (cf. Blyholder, et al. (12)). In particular, the present results show no indication of the change in reaction order in  $[O_2]$  suggested by the two site theory (12).

In Fig.7, the  $R_e$  values are compared with previous studies of soot and carbon black oxidation at  $[O_2] = 3.5 \times 10^{17} \text{ cm}^{-3}$ . The data are those of NSC (10), Park and Appelton (11), PA, on carbon black oxidation in a shock tube (the PA and NSC results are identical), and of Lee, Thring, and Beér (13), LTB, on soot oxidation in an  $O_2$ -rich flame. At this  $[O_2]$  and higher, R16 and CSC oxidation are significantly slower than that of previously studied carbon blacks and soot. An "activation energy" of  $\approx 170 \text{ kJ}$  is consistent with all of the measurements. At lower  $[O_2]$  ( $\approx 2 \times 10^{14}$ ), the present results are compared with those of Rosner and

Allendorf (14), (RA), and NSC in Fig. 8. At this low  $[O_2]$ , RA's measurements on isotropic and pyrolytic graphite bracket those predicted by NSC and those measured in the present work. The "turnover" in the reactivity coefficient values predicted by NSC and observed by RA may be present for R16, but it is not suggested by the CSC data.

Figures 9 and 10 display the probability of reaction,  $\bar{\tau}$ , per  $O_2$ -surface collision calculated using kinetic theory to determine the number of collisions/s per unit surface area and the measured  $R_p$  values. The data of RA on pyrolytic graphite over a range of low  $[O_2]$  at  $\approx 1500$  K are shown for comparison in Fig. 9. In Fig. 10,  $\bar{\tau}$  for R16 and CSC is shown for most of the wide range of  $[O_2]$  covered in this work at the extremes of the temperature ranges investigated. The low reactivity of these carbon blacks translates into collision efficiencies as low as  $\approx 1 \times 10^{-6}$  at  $[O_2] = 1 \times 10^{18} \text{ cm}^{-3}$  and as high as  $\approx 4 \times 10^{-3}$  at  $[O_2] = 1 \times 10^{15} \text{ cm}^{-3}$ . These values are comparable to those for graphitic carbons.

Thus, the present results indicate low reactivity for R16 and CSC for  $[O_2]$  values of practical interest. The complex  $[O_2]$ -dependence of  $R_p$  required by NSC kinetics is not observed over the temperature range studied, despite extremely wide variations in  $[O_2]$ . The data show no significant differences which can be attributed to metallic content. We speculate that the high sulfur content in these carbon blacks may be the cause of their low reactivity and the failure of the two site model to describe their oxidation kinetics. The sulfur content (mole fraction  $\approx 40$  ppm) may be sufficient to poison potential metallic catalytic sites (on a molar basis, sulfur is  $\approx 20$  times more abundant than metals in R16 and 10 times more in CSC) as well as to interfere with active sites in both carbon blacks. If correct, this speculation suggests that it is important to avoid sulfur contamination where carbonaceous burnout at "low" temperature is desired.

#### REFERENCES

1. Neoh, K.G., Howard, J.B., and Sarofim, A.F., in Particulate Carbon: Formation During Combustion, D.C. Siegl and G.W. Smith, Eds., Plenum Press, New York, (1981), p. 261.
2. Page, F.M. and Ates, F., in Evaporation and Combustion of Fuels, J.T. Zung, Ed., Advances in Chemistry 166, American Chemical Society, Washington, D.C. (1978), p. 190.
3. Fenimore, C.P. and Jones, G.W., J. Phys. Chem. 71, 593 (1967).
4. Laurendeau, N.M., Prog. Energy Combust. Sci. 4, 221 (1978).
5. Fontijn, A. and Felder, W., in Reactive Intermediates in the Gas Phase: Generation and Monitoring, D.W. Setser, Ed., Academic Press, New York, (1979) Chap. 2.
6. Lowell, S. Introduction to Powder Surface Area, Wiley-Interscience, New York (1979).
7. Mulcahy, M.F.R. and Smith, I.W., Pure and Appl. Chem. 19, 81 (1969)
8. Essenhigh, R.H., in Chemistry of Coal Utilization, 2nd Supplementary Volume, M.A. Elliott, Ed., Wiley, New York, (1981) Chap. 19.
9. Smith, I.W., Combust. Flame 17, 303 (1971)

10. Nagle, J. and Strickland-Constable, R.F., Proceedings of the Fifth Conference on Carbon, Volume 1, Macmillan, New York (1962), p. 154.
11. Park, C. and Appelton, J.P., Combust. Flame **20**, 369 (1973).
12. Blyholder, G., Binford, J.S., Jr., and Eyring, H., J. Phys. Chem. **62**, 263 (1958).
13. Lee, K.B., Thring, M.W., and Beer, J.M., Combust. Flame **6**, 137 (1962).
14. Rosner, D.E. and Allendorf, H.D., AIAA J. **6**, 650 (1968).

TABLE I. PHYSICAL AND CHEMICAL PROPERTIES OF CARBON BLACKS<sup>a</sup>

Trade Name	Mean Particle Diam. (nm)	BET (N <sub>2</sub> ) Surface Area (m <sup>2</sup> g <sup>-1</sup> )	Volatiles (wt %)	Metal Content (wt %) <sup>c</sup>	Ash (wt %)	Sulfur (wt %)
Raven 16	61	25 (29 <sup>b</sup> )	0.9	0.1 <sup>c</sup>	0.098	1.67
Conductex SC	20	220 (190 <sup>b</sup> )	1.5	0.08 <sup>c</sup>	0.075	0.85

<sup>a</sup> Data supplied by manufacturer.

<sup>b</sup> Measured in this work.

<sup>c</sup> Metallic impurities, wt. %:

	R16	CSC
I Mn, Mg, Al, Ti	0.007	0.008
Fe	0.045	0.005
Na	0.021	0.047
Ca	0.025	0.016

TABLE II. EXTERNAL SURFACE REACTIVITY FOR CARBON BLACK OXIDATION BY O<sub>2</sub>

$$\log_{10} R_e = \log_{10} R_0 + n \log_{10} [O_2]$$

Carbon Black	T (K)	$\log_{10} R_0$ (g cm <sup>-2</sup> s <sup>-1</sup> [O <sub>2</sub> ] <sup>-n</sup> )	n	[O <sub>2</sub> ] range (10 <sup>16</sup> cm <sup>-3</sup> )
Raven 16	1300	-16.3 ± 0.5 <sup>a</sup>	0.62 ± 0.04 <sup>a</sup>	0.02 - 158
	1400	-16.5 ± 2.0	0.64 ± 0.12	2.0 - 104
	1470	-16.1 ± 1.3	0.66 ± 0.10	0.02 - 98
	1580	-14.9 ± 1.7	0.59 ± 0.10	0.12 - 177
	1680	-15.1 ± 1.0	0.61 ± 0.07	0.03 - 154
Conductex SC	1410	-18.6 ± 0.5	0.76 ± 0.13	0.03 - 200
	1580	-18.8 ± 1.1	0.82 ± 0.17	0.02 - 130
	1650	-14.2 ± 1.4	0.57 ± 0.09	0.02 - 75

<sup>a</sup> One standard deviation

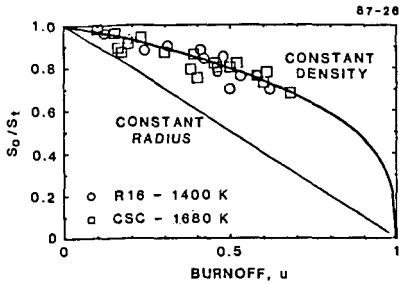


FIGURE 1 VARIATION OF CARBON BLACK SURFACE AREA WITH BURNOFF

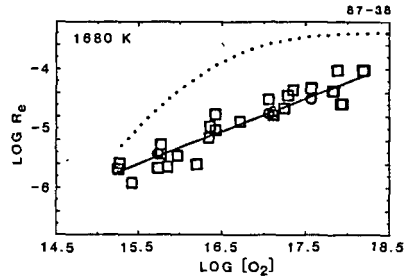


FIGURE 4 R16 OXIDATION BY  $O_2$   
 □ - gc data; ○ - scattering data;  
 ... -NSC (10) prediction

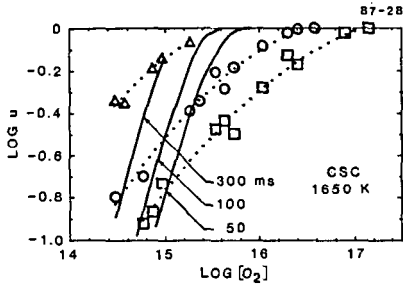


FIGURE 2 BURNOFF OF CSC AT 1650 K  
 Residence times: □ - 50 ms; ○ - 100 ms;  
 Δ - 300 ms. Solid lines are NSC (10)  
 predictions.

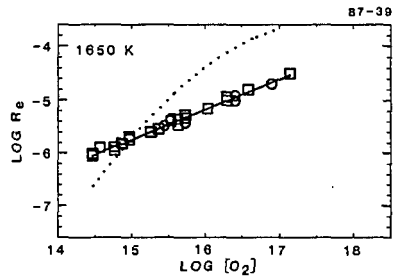


FIGURE 5 CSC OXIDATION BY  $O_2$   
 □ - gc data; ○ - scattering data;  
 ... -NSC (10) prediction

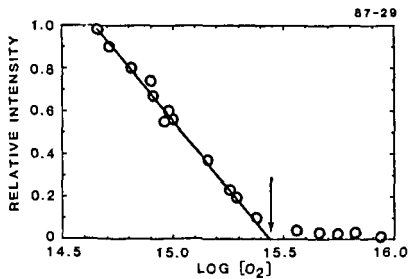


FIGURE 3 LASER SCATTERING MEASUREMENT  
 OF CSC OXIDATION AT 1650 K  
 $[O_2] = 2.8 \times 10^{15}$  (arrow),  $t_0 = 380$  ms

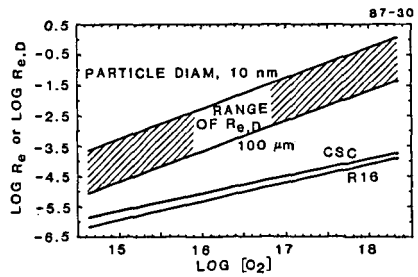
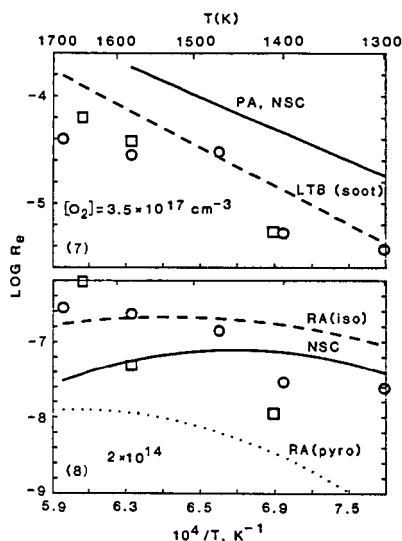


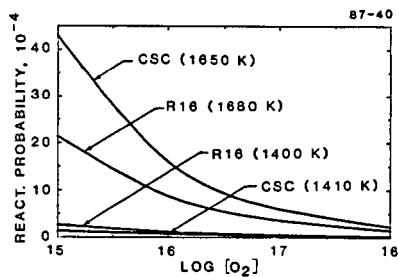
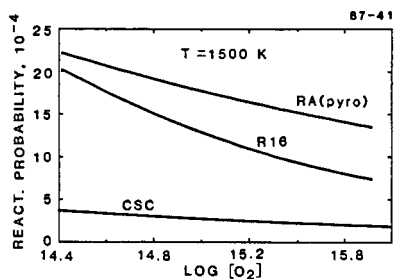
FIGURE 6 COMPARISON OF DIFFUSION-LIMITED  
 REACTIVITY WITH OBSERVED VALUES AT 1700K

87-44



FIGURES 7 and 8 TEMPERATURE DEPENDENCE OF CARBON BLACK OXIDATION

o - R16;  $\square$  -CSC; NSC - Nagle and Strickland-Constable (10); PA - Park and Appelton (11); LTB -Lee, Thring and Beer (13); RA - Rosner and Allendorf (14) for isotropic (iso) and pyrolytic (pyro) graphite



FIGURES 9 and 10 DEPENDENCE OF REACTION PROBABILITY ON  $[\text{O}_2]$

RA(pyro) - results of Rosner and Allendorf (14) on pyrolytic graphite.